NUMERICAL INVESTIGATION OF STATIC AND DYNAMIC STRESSES IN SPUR GEAR MADE OF COMPOSITE MATERIAL

Asst. Prof. MOHAMMAD Q. ABDULLAH & THAR M. BADRI

ABSTRACT

In this current work, ***Purpose***; to clearly the fundamental idea for constructing a design and investigation of spur gear made of composite material its comes from the combination of (high speeds, low noise, oil-les running, light weight, high strength, and more load capability) encountered in modern engineering applications of the gear drives, when the usual metallic gear cannot too overwhelming these combinations.

An analyzing of stresses and deformation under static and dynamic loading for spur gear tooth by finite element method with isoparametric eight-nodded in total of 200 brick element with 340 nods in three degree of freedom per node was selected for this analysis. This is responsible for the catastropic failure studying of spur gear made of composite material. Also obtain the natural frequencies and the mode shape of the composite tooth under (concentrated and or moving on surface profile) load of one half sinusoidal type impulse for two types of composite materials (Glasses/Epoxy & Graphite/Epoxy) and they are compared with the mild steel gear values.

The appearances that improve the successfully of composite gear in the weight, stiffness, load capability, and dynamic behavior respect to the mild steel, which is found that composite materials may also be thought of as a material for power transmission gearing, from a stress point of view.

الخلاصة

في الدراسة الحالية و التي تبحث في الفكرة ا ستغلال المواد المركبة لصناعة التروسس و التي استنبطت من خلال متطلبات تصاميم التروسس الحديثة وهي (السرع العالية، اقل ضوضاء، اقل مستوى لتزييت، وزن اقل، صلابة عالية، مع قدرة عمل افضل) والتي لا تستطيع ان تحتويها التروسس المعدنية. من خلال اجراء تحليل لاجهادات و التشوهات الحاصلة لمسنن الاصم تحت تاثير ظروف الاستخدام القوى الساكنة والمتحركة باستخدام طريقة العناصر المحددة (FEM) باستخدام 200 عنصرو340 نقطة لثلاث درجات من الحرية للنقطة الواحدة. كذلك تم دراسة الفشل المرتبط بنظام بناء المواد المركبة وبنفس ظروف التحميل السابقة ووجد ان (الترددات الطبيعية وشكل الطوار). للمسنن المصنع من المواد المركبة تحت تاثير قوة متمركزة واخرا متحركة على امتدا سطح المسن اقل مماهو عليه في المسنن المعدني.

ان الدراسة المفصلة بالجزئين العملي والنظري اثبتت ان التروس المصنعة من المواد المركبة اكثر قدرة على تحمل الاجهادات باتجاه الالياف من التروس المعدنية و اصبح بالامكان من استخدام المواد المركبة كبديل عن المعادن.

Keywords: composite, spur gear, glasses/graphite/epoxy, numerical static and dynamic stresses analysis, aircrafts gear pump.

INTRODUCTION

In the past century, there have been major developments in the technology of power transmission by gears. One particular field of research which plays a key role by assessment of mesh stiffness of orthotropic material gear because of, it can be rebuilt the macrostructures of materials to create new mechanical properties of combination of (low noise, oil-les running, light weight, and high strength) using for power transmission.

So the metallic gear is; heavy but difficult to use oil-less condition. Also the plastic gear; less in weight but low loading capability, and weaker impact loading, Thus composite gear are attention (to meet market requirement)**[Toshiki H. 2006]**, Which is a part of orthotropic material and achieved their entire gear problem because it lighter materials are desired or required without sacrificing strength. They have even become essential for many gear applications.

In a general sense, the word composite means constituted of two or more different parts in practice, the term of composite is used in a more restrictive sense, as a material constituted by the assemblage of two or more materials of different natures with complementary properties leading to a material which have better properties than the properties of the composite components considered separately **[Jean-Marie Berthelot 2003]**. So composite preferred in places because of:-

1) Two or more materials combined on a ***macroscopic*** scale to form a useful material.
2) Ideal for structural applications ***"high strength-to-weight and stiffness-to-weight ratio"***.
3) Conventional composites limited to in-plane distributed loads.
4) The properties of composite materials are result from:

a -The properties of constituent materials,

b- Their geometrical distribution,

c- Their interaction.

Some transmission gears make use of composite materials in many different places such as watches, instruments, washing machine, gear pumps, etc. It has been reported **[Vijayarangan and N. Ganesan 1992]** that the life of stainless-steel gear pump was prolonged when the gear made from glass-fiber reinforced epoxy was exchanged and when an injection moulding compound, reinforced with 30% by weight carbon fibers, was used for the gears. This pump recorded 1000 hours of extra life. Because of the overwhelming advantages of composite materials and its existing use for high power or kinematic applications, that lead to be interested to know the feasibility of usage of composite materials for power transmission gearing. The literatures available on metallic (isotropic) gears both on experimental and on theoretical studies is enormous. However, the authors could trace very little literature about composite gears.

But here will be investigate a practical model of composite material and studying its behavior comprehensively, {numerically by FEM, when an attempt has been made to study ***the variation of tensile and compressive stresses***, ***on the load and unloaded sides of tooth surface***, which are responsible for the catastropic failure of gear tooth made of composite material}, and then made a comparison between the composite spur gear with isotropic one.

The finite element method [FEM] is a numerical technique in which governing equations are represented in matrix form and as such are well suited to solution by advance mathematical programming using [maple calculator package Ver. (11)].

From the results obtained by analyzing a spur gear made of orthotropic material, which

is found that these composite materials may also be thought of as a material for power transmission gearing, from a stress point of view.

FINITE ELEMENT MODELING OF COMPOSITE GEAR TOOTH SECTOR

Since the three dimensions, namely the tooth height, tooth thickness and tooth face width, of a gear tooth in three mutually perpendicular directions are comparable with each other it is more appropriate to use ***3D modeling***. Table 1 show the standard parameters used in this work. The gear tooth sector developed in 3D figure was extrapolated in the perpendicular (Z-axis) direction as it is only a spur gear, the same configuration as in the front exists all through the Z-axis. ***A fine mesh closer to the root section was chosen to get better results of root stresses in total of 200 elements with 340 nodes were used for the analysis*** Fig.1. Each gear tooth sector subtends to an angle of 360˚/z, where z is the number of teeth in the gear. This is chosen for ***cyclic symmetry*** is applied [**S. Mohamed Nabi & N. Ganesan, 1993**] later on.

An external normal force (F) of amplitude (245.25 N) is applied at a single point in the tip of the tooth (concentrated loads) this uniformly distributed load was lumped at the nodes. The value of the applied force is selected such that the expected maximum stress is less than the yield strength of the composite materials and mild steel (Hereafter called as Gl/Ep, Gr/Ep and Ms, respectively) present in the Table 2.

$$\left.\begin{aligned}
N_1 &= \tfrac{1}{2}(1-\zeta)(1-\eta)(1-\tau)\\
N_2 &= \tfrac{1}{2}(1-\zeta)(1+\eta)(1-\tau)\\
N_3 &= \tfrac{1}{2}(1+\zeta)(1-\eta)(1-\tau)\\
N_4 &= \tfrac{1}{2}(1+\zeta)(1+\eta)(1-\tau)\\
N_5 &= \tfrac{1}{2}(1-\zeta)(1-\eta)(1+\tau)\\
N_6 &= \tfrac{1}{2}(1-\zeta)(1+\eta)(1+\tau)\\
N_7 &= \tfrac{1}{2}(1+\zeta)(1-\eta)(1+\tau)\\
N_8 &= \tfrac{1}{2}(1+\zeta)(1+\eta)(1+\tau)
\end{aligned}\right\} \quad (2)$$

Displacement and Force Fields

FORMULATION OF CHARACTERISTICS MATRICES AND VECTORS

Consider three coordinates x, y and z to be associated with element in Cartesian plane as shown in Fig. 1. It is useful to employ a local system which is simple, unique and independent of the global system, such a system is known as an intrinsic system and its coordinates are the intrinsic coordinate's ζ, η and τ.

The problem now reduces to one of obtaining the equation of the transformation from the Cartesian plane. It can be assumed that x, y and z is field functions defined as follows:

$$\left.\begin{aligned}
X(\zeta,\eta,\tau) &= \textstyle\sum_{i=1}^{n=8} x_i N_i\ (\zeta,\eta,\tau)\\
y(\zeta,\eta,\tau) &= \textstyle\sum_{i=1}^{n=8} y_i N_i\ (\zeta,\eta,\tau)\\
z(\zeta,\eta,\tau) &= \textstyle\sum_{i=1}^{n=8} z_i N_i\ (\zeta,\eta,\tau)
\end{aligned}\right\} \quad (1)$$

In which x_i, y_i and z_i are nodal coordinates and $N_i(\zeta, \eta, \tau)$ are functions of ζ ,η and τ called shape function .For any point in the intrinsic plane with known values of ζ ,η and τ the Cartesian x ,y and z coordinates can be found once the functions Ni(ζ , η , τ) are known.

The nodal displacement vector {δ} and the force vector {F} can be defined as follows:-

$$\left.\begin{aligned}
\{\delta\} &= \{u_1 v_1 w_1 u_2 v_2 w_2 \dots\dots\dots u_8 v_8 w_8\}\\
\{F\} &= \{fx_1 fy_1 fz_1 fx_2 fy_2 fz_2 \dots\dots\dots fx_8 fy_8 fz_8\}
\end{aligned}\right\} \quad (3)$$

The displacements components at any point can be expressed in terms of displacements and shape function:-

$$\left.\begin{aligned}
u(x,y,z) &= \textstyle\sum_{i=1}^{n=8} u_i N_i\ (x,y,z) \qquad u(\zeta,\eta,\tau) = \textstyle\sum_{i=1}^{n=8} u_i N_i\ (\zeta,\eta,\tau)\\
v(x,y,z) &= \textstyle\sum_{i=1}^{n=8} v_i N_i\ (x,y,z) \qquad v(\zeta,\eta,\tau) = \textstyle\sum_{i=1}^{n=8} v_i N_i\ (\zeta,\eta,\tau)\\
w(x,y,z) &= \textstyle\sum_{i=1}^{n=8} w_i N_i\ (x,y,z) \qquad w(\zeta,\eta,\tau) = \textstyle\sum_{i=1}^{n=8} w_i N_i\ (\zeta,\eta,\tau)
\end{aligned}\right\} \quad (4)$$

Where, u(x,y,z) ,v(x,y,z,) ,w(x,y,z) represents the displacement components at any point

(x,y,z) inside the element, $N_i(x,y,z)$ represents the shape function at node, i and n represents the number of element nodes. Finally, the displacement vector {q} at any point (x, y and z) inside the element can be defined as follows:-

$$\{q\} = \begin{bmatrix} N_1 & 0 & 0 & N_2 & 0 & 0 & \dots N_8 & 0 & 0 \\ 0 & N_1 & 0 & 0 & N_2 & 0 & \dots 0 & N_8 & 0 \\ 0 & 0 & N_1 & 0 & 0 & N_2 & \dots 0 & 0 & N_8 \end{bmatrix} \{\delta\}$$

$$\text{Hence } \{q\} = [N]\{\delta\} \quad (5)$$

Strain Field

From the strain-displacement relations it is very useful to form the shape functions expressed in terms of intrinsic coordinates (ζ, η and τ) for initial calculation.

$$\begin{Bmatrix} \varepsilon_x \\ \varepsilon_y \\ \varepsilon_z \\ \gamma_{xy} \\ \gamma_{xz} \\ \gamma_{yz} \end{Bmatrix} = \begin{Bmatrix} \frac{\partial u}{\partial x} \\ \frac{\partial v}{\partial y} \\ \frac{\partial w}{\partial z} \\ \frac{\partial u}{\partial y} + \frac{\partial v}{\partial x} \\ \frac{\partial u}{\partial z} + \frac{\partial w}{\partial x} \\ \frac{\partial v}{\partial z} + \frac{\partial w}{\partial y} \end{Bmatrix} = [J] \begin{Bmatrix} \frac{\partial u}{\partial \zeta} \\ \frac{\partial v}{\partial \eta} \\ \frac{\partial w}{\partial \tau} \\ \frac{\partial u}{\partial \eta} + \frac{\partial v}{\partial x} \\ \frac{\partial u}{\partial z} + \frac{\partial w}{\partial x} \\ \frac{\partial v}{\partial z} + \frac{\partial w}{\partial y} \end{Bmatrix} \quad (6)$$

Here [J] is the Jacobean matrix.

Since that the nodal displacement vector in terms of intrinsic co-ordinates is;

$$\frac{\partial u}{\partial \zeta} = \left[\frac{\partial N_1}{\partial \zeta} \quad 0 \quad 0 \quad \frac{\partial N_2}{\partial \zeta} \quad 0 \quad 0 \dots \dots \dots \quad \frac{\partial N_8}{\partial \zeta} \quad 0 \quad 0\right]\{\delta\}$$

$$\frac{\partial v}{\partial \eta} = \left[0 \quad \frac{\partial N_1}{\partial \eta} \quad 0 \quad 0 \quad \frac{\partial N_2}{\partial \eta} \quad 0 \dots \dots \dots \quad 0 \quad \frac{\partial N_8}{\partial \eta} \quad 0\right]\{\delta\}$$

$$\frac{\partial w}{\partial \tau} = \left[0 \quad 0 \quad \frac{\partial N_1}{\partial \tau} \quad 0 \quad 0 \quad \frac{\partial N_2}{\partial \tau} \dots \dots \dots \quad 0 \quad 0 \quad \frac{\partial N_8}{\partial \tau}\right]\{\delta\}$$

And

$$\frac{\partial u}{\partial \eta} + \frac{\partial v}{\partial \zeta} = \left[\frac{\partial N_1}{\partial \eta} \quad \frac{\partial N_1}{\partial \zeta} \quad 0 \quad \frac{\partial N_2}{\partial \eta} \quad \frac{\partial N_2}{\partial \zeta} \quad 0 \dots \dots \dots \quad \frac{\partial N_8}{\partial \eta} \quad \frac{\partial N_8}{\partial \zeta} \quad 0\right]\{\delta\}$$

$$\frac{\partial u}{\partial \tau} + \frac{\partial w}{\partial \zeta} = \left[\frac{\partial N_1}{\partial \tau} \quad 0 \quad \frac{\partial N_1}{\partial \zeta} \quad \frac{\partial N_2}{\partial \tau} \quad 0 \quad \frac{\partial N_2}{\partial \zeta} \dots \dots \dots \quad \frac{\partial N_8}{\partial \tau} \quad 0 \quad \frac{\partial N_8}{\partial \zeta}\right]\{\delta\}$$

$$\frac{\partial v}{\partial \tau} + \frac{\partial w}{\partial \eta} = \left[0 \quad \frac{\partial N_1}{\partial \tau} \quad \frac{\partial N_1}{\partial \eta} \quad 0 \quad \frac{\partial N_2}{\partial \tau} \quad \frac{\partial N_2}{\partial \eta} \dots \dots \dots \quad 0 \quad \frac{\partial N_8}{\partial \tau} \quad \frac{\partial N_8}{\partial \eta}\right]\{\delta\}$$

Hence, it can be deduced that; $\underset{6\times1}{\{\varepsilon\}} = \underset{6\times24}{[B]}\ \underset{24\times1}{\{\delta\}}$, Where {ε} is a strain vector, {δ} is the nodal displacement vector and [B] is the strain displacement matrix all of them in terms of intrinsic co-ordinates.

$$\begin{bmatrix} \frac{\partial u}{\partial \zeta} \\ \frac{\partial v}{\partial \eta} \\ \frac{\partial w}{\partial \tau} \\ \frac{\partial u}{\partial \eta} + \frac{\partial v}{\partial \zeta} \\ \frac{\partial u}{\partial \tau} + \frac{\partial w}{\partial \zeta} \\ \frac{\partial v}{\partial \tau} + \frac{\partial w}{\partial \eta} \end{bmatrix} = \begin{bmatrix} \frac{\partial N_1}{\partial \zeta} & 0 & 0 & \frac{\partial N_2}{\partial \zeta} & 0 & 0 & \dots & \frac{\partial N_8}{\partial \zeta} & 0 & 0 \\ 0 & \frac{\partial N_1}{\partial \eta} & 0 & 0 & \frac{\partial N_2}{\partial \eta} & 0 & \dots & 0 & \frac{\partial N_8}{\partial \eta} & 0 \\ 0 & 0 & \frac{\partial N_1}{\partial \tau} & 0 & 0 & \frac{\partial N_2}{\partial \tau} & \dots & 0 & 0 & \frac{\partial N_8}{\partial \tau} \\ \frac{\partial N_1}{\partial \eta} & \frac{\partial N_1}{\partial \zeta} & 0 & \frac{\partial N_2}{\partial \eta} & \frac{\partial N_2}{\partial \zeta} & 0 & \dots & \frac{\partial N_8}{\partial \eta} & \frac{\partial N_8}{\partial \zeta} & 0 \\ \frac{\partial N_1}{\partial \tau} & 0 & \frac{\partial N_1}{\partial \zeta} & \frac{\partial N_2}{\partial \tau} & 0 & \frac{\partial N_2}{\partial \zeta} & \dots & \frac{\partial N_8}{\partial \tau} & 0 & \frac{\partial N_8}{\partial \zeta} \\ 0 & \frac{\partial N_1}{\partial \tau} & \frac{\partial N_1}{\partial \eta} & 0 & \frac{\partial N_2}{\partial \tau} & \frac{\partial N_2}{\partial \eta} & \dots & 0 & \frac{\partial N_8}{\partial \tau} & \frac{\partial N_8}{\partial \eta} \end{bmatrix} \begin{Bmatrix} u_1 \\ v_1 \\ w_1 \\ u_2 \\ v_2 \\ w_2 \\ \vdots \\ u_8 \\ v_8 \\ w_8 \end{Bmatrix} \quad (7)$$

That led to differentiation the shape function with respect to intrinsic coordinate as follow;

$$\frac{\partial N_1}{\partial \zeta} = -\frac{1}{2}(1-\eta)(1-\tau)$$
$$\frac{\partial N_2}{\partial \zeta} = -\frac{1}{2}(1+\eta)(1-\tau)$$
$$\frac{\partial N_3}{\partial \zeta} = \frac{1}{2}(1-\eta)(1-\tau)$$
$$\frac{\partial N_4}{\partial \zeta} = \frac{1}{2}(1+\eta)(1-\tau)$$
$$\frac{\partial N_5}{\partial \zeta} = -\frac{1}{2}(1-\eta)(1+\tau)$$
$$\frac{\partial N_6}{\partial \zeta} = -\frac{1}{2}(1+\eta)(1+\tau)$$
$$\frac{\partial N_7}{\partial \zeta} = \frac{1}{2}(1-\eta)(1+\tau)$$
$$\frac{\partial N_8}{\partial \zeta} = \frac{1}{2}(1+\eta)(1+\tau)$$

$$\frac{\partial N_1}{\partial \eta} = -\frac{1}{2}(1-\zeta)(1-\tau)$$
$$\frac{\partial N_2}{\partial \eta} = \frac{1}{2}(1-\zeta)(1-\tau)$$
$$\frac{\partial N_3}{\partial \eta} = -\frac{1}{2}(1+\zeta)(1-\tau)$$
$$\frac{\partial N_4}{\partial \eta} = \frac{1}{2}(1+\zeta)(1-\tau)$$
$$\frac{\partial N_5}{\partial \eta} = -\frac{1}{2}(1-\zeta)(1+\tau)$$
$$\frac{\partial N_6}{\partial \eta} = \frac{1}{2}(1-\zeta)(1+\tau)$$
$$\frac{\partial N_7}{\partial \eta} = -\frac{1}{2}(1+\zeta)(1+\tau)$$
$$\frac{\partial N_8}{\partial \eta} = \frac{1}{2}(1+\zeta)(1+\tau)$$

$$\frac{\partial N_1}{\partial \tau} = -\frac{1}{2}(1-\zeta)(1-\eta)$$
$$\frac{\partial N_2}{\partial \tau} = -\frac{1}{2}(1-\zeta)(1+\eta)$$
$$\frac{\partial N_3}{\partial \tau} = -\frac{1}{2}(1+\zeta)(1-\eta)$$
$$\frac{\partial N_4}{\partial \tau} = -\frac{1}{2}(1+\zeta)(1+\eta)$$
$$\frac{\partial N_5}{\partial \tau} = \frac{1}{2}(1-\zeta)(1-\eta)$$
$$\frac{\partial N_6}{\partial \tau} = \frac{1}{2}(1-\zeta)(1+\eta)$$
$$\frac{\partial N_7}{\partial \tau} = \frac{1}{2}(1+\zeta)(1-\eta)$$
$$\frac{\partial N_8}{\partial \tau} = \frac{1}{2}(1+\zeta)(1+\eta) \quad (8)$$

The Stress-Strain Matrix

To determine the elasticity or (stress-strain) matrix from the normal stresses and the shear stresses relationships where E_1, E_2, E_3 are the elastic modules, G_{12}, G_{23}, G_{13}, are shear modules and υ_{12}, υ_{23}, υ_{13} are Poisson's ratio in the L, T, Z directions of the fiber and LT, TZ and ZL planes. ***"Assuming that the reinforcing fibers in an element are all in a radial direction"***:-

$$\left.\begin{aligned} \varepsilon_x &= \frac{\sigma_x}{E_1} - \upsilon_{12}\frac{\sigma_y}{E_2} - \upsilon_{13}\frac{\sigma_z}{E_3} & \tau_{xy} &= \gamma_{xy}G \\ \varepsilon_y &= -\upsilon_{21}\frac{\sigma_x}{E_1} + \frac{\sigma_y}{E_2} - \upsilon_{23}\frac{\sigma_z}{E_3} & \tau_{xz} &= \gamma_{xz}G \\ \varepsilon_z &= -\upsilon_{31}\frac{\sigma_x}{E_1} - \upsilon_{32}\frac{\sigma_y}{E_2} + \frac{\sigma_z}{E_3} & \tau_{yz} &= \gamma_{yz}G \end{aligned}\right\} \quad (9)$$

Hence $\{\varepsilon\} = [S]\{\sigma\}$, where $\{\varepsilon\}$ is strain vector, $\{\sigma\}$ is stresses vector, and [S]is the compliance matrix. But the compliance matrix it is the inverse of the elasticity matrix, so $[S]^{-1} = [D]$. Or;

$$\begin{Bmatrix}\sigma_x\\ \sigma_y\\ \sigma_z\\ \tau_{xy}\\ \tau_{xz}\\ \tau_{yz}\end{Bmatrix} = \begin{bmatrix} C_{11} & C_{12} & C_{13} & o & o & o \\ C_{12} & C_{22} & C_{23} & o & o & o \\ C_{13} & C_{23} & C_{33} & o & o & o \\ o & o & o & C_{44} & o & o \\ o & o & o & o & C_{55} & o \\ o & o & o & o & o & C_{66} \end{bmatrix} \begin{Bmatrix}\varepsilon_x\\ \varepsilon_y\\ \varepsilon_z\\ \gamma_{xy}\\ \gamma_{xz}\\ \gamma_{yz}\end{Bmatrix} \quad (10)$$

Where [D] is the elasticity or (stress-strain) matrix ***for an orthotropic material.***

Where C_{ij} is the elasticity constant explaining by the relation down as follows ;

$$\begin{aligned} C11 &= E_1(1-\upsilon_{23}\upsilon_{32})/(1-(\upsilon_{12}\upsilon_{21}-\upsilon_{32}\upsilon_{23}-\upsilon_{31}\upsilon_{13})-2\upsilon_{13}\upsilon_{32}\upsilon_{21}) \\ C12 &= E_1(\upsilon_{21}+\upsilon_{23}\upsilon_{32})/(1-(\upsilon_{12}\upsilon_{21}-\upsilon_{32}\upsilon_{23}-\upsilon_{31}\upsilon_{13})-2\upsilon_{13}\upsilon_{32}\upsilon_{21}) \\ C13 &= E_1(\upsilon_{31}+\upsilon_{23}\upsilon_{32})/(1-(\upsilon_{12}\upsilon_{21}-\upsilon_{32}\upsilon_{23}-\upsilon_{31}\upsilon_{13})-2\upsilon_{13}\upsilon_{32}\upsilon_{21}) \\ C22 &= E_2(1-\upsilon_{13}\upsilon_{31})/(1-(\upsilon_{12}\upsilon_{21}-\upsilon_{32}\upsilon_{23}-\upsilon_{31}\upsilon_{13})-2\upsilon_{13}\upsilon_{32}\upsilon_{21}) \\ C23 &= E_2(\upsilon_{32}+\upsilon_{12}\upsilon_{31})/(1-(\upsilon_{12}\upsilon_{21}-\upsilon_{32}\upsilon_{23}-\upsilon_{31}\upsilon_{13})-2\upsilon_{13}\upsilon_{32}\upsilon_{21}) \\ C33 &= E_3(1-\upsilon_{12}\upsilon_{21})/(1-(\upsilon_{12}\upsilon_{21}-\upsilon_{32}\upsilon_{23}-\upsilon_{31}\upsilon_{13})-2\upsilon_{13}\upsilon_{32}\upsilon_{21}) \\ C44 &= G_{12} \\ C55 &= G_{23} \\ C66 &= G_{31} \end{aligned} \quad (11)$$

***properties achieved by simple tensile test the entire elasticity constant in terms of mechanical* Stress Field**

Referring to the Eq. (10) it can be deduced that:-

$$\{\sigma\} = [D]\{\varepsilon\}$$

Where {σ} is the stress vector,

From Eq. (7) and Eq. (10) it can be found that:-

$$\{\sigma\} = [D][B]\{\delta\} \quad (12)$$

Formulation of the Transformation Matrix

The fiber orientation angle (α) measured from ***the vertical direction (X -axis)*** is given as $\alpha = \tan^{-1}(XX/YY)$, where XX and YY are the X and Y co-ordinates of the geometric centre of any element under consideration. The transformation of elastic properties E_L, E_T, E_Z, G_{LT}, G_{LZ}, G_{TZ}, υ_{LT}, υ_{lZ}, υ_{TZ} with

respect to local x, y, z co-ordinates were performed using an appropriate transformation matrix. The transformation matrix used in this case is:-

$$[T] = \begin{bmatrix} S^2 & C^2 & 0 & -2CS & 0 & 0 \\ C^2 & S^2 & 0 & 2CS & 0 & 0 \\ 0 & 0 & 1 & 0 & 0 & 0 \\ CS & CS & 0 & S^2-C^2 & 0 & 0 \\ 0 & 0 & 0 & 0 & S & -C \\ 0 & 0 & 0 & 0 & C & S \end{bmatrix}$$

Where $S = \sin\alpha$ and $C = \cos\alpha$. (13)

Formulation of Element Stiffness Matrix

Three degrees of freedom per node, namely displacements u, v, w in the X, Y, and Z co-ordinates were assumed. The Cartesian co-ordinates x, y and z describing the elemental continuum, the intrinsic co-ordinates ζ , η and τ ranging from -1 to $+1$ on element boundaries and the intrinsic node numbering are all shown in Fig. 1.

The element stiffness matrix is found from the ***total potential energy*** of the element **P**. This energy can be expressed as follows:-

$$P = U - W$$

Where U is the strain energy can be shown as: -

$$U = \frac{1}{2}\iiint_{element}\{\sigma\}^T\{\varepsilon\}\,dx\,dy\,dz$$

Work done by the external force is:-

$$W = \{\delta\}^T\{F\}$$

From eq. (12), it is clear that:-

$$\{\sigma\}^* = \{\delta\}^T[B]^T[D]^*$$

Thus the composite material stiffness matrix [D*] was obtained as:-

$$[D^*] = [T]\,[D]\,[T]^T \qquad (14)$$

Hence,

$$U = \frac{1}{2}\iiint_{element}\{\delta\}^T\,[B]^T[D^*][B]\{\delta\}\,dx\,dy\,dz$$

Then

$$P = \frac{1}{2}\{\delta\}^T\left[\iiint_{element}[B]^T[D^*][B]\,dx\,dy\,dz\right]\{\delta\} - \{\delta\}^T\{F\}$$

Apply the minimum total potential energy theorem:- $\frac{\partial P}{\partial\{\delta\}} = 0$

$$\left[\iiint_{element}[B]^T[D^*][B]\,dx\,dy\,dz\right]\{\delta\} = \{F\}$$

But; - [K] $\{\delta\}$= {f}, then finally the element stiffness matrix is:-

$$[K] = \iiint_{element}[B]^T[D^*][B]\,dx\,dy\,dz$$

By converting the Cartesian coordinate to intrinsic coordinate, the eq. become:-

$$\left[\underset{\sim}{K}_{24\times24}\right] = \iiint_{element}\left[\underset{\sim}{B}_{24\times6}\right]^T\left[\underset{\sim}{D^*}_{6\times6}\right]\left[\underset{\sim}{B}_{6\times24}\right]|J|\,d\zeta\,d\eta\,d\tau \qquad (15)$$

The integration in Eq. (15) is evaluated numerically using the modified Gauss-quadratic. where [J] is the Jacobean matrix

$$\begin{Bmatrix} \frac{\partial u}{\partial\zeta} \\ \frac{\partial v}{\partial\eta} \\ \frac{\partial w}{\partial\tau} \\ \frac{\partial u}{\partial\eta}+\frac{\partial v}{\partial\zeta} \\ \frac{\partial u}{\partial\tau}+\frac{\partial w}{\partial\zeta} \\ \frac{\partial v}{\partial\tau}+\frac{\partial w}{\partial\eta} \end{Bmatrix} = \begin{bmatrix} \frac{\partial X}{\partial\zeta} & \frac{\partial Y}{\partial\zeta} & \frac{\partial Z}{\partial\zeta} & - & - & - & - & - & - \\ - & - & - & \frac{\partial X}{\partial\eta} & \frac{\partial Y}{\partial\eta} & \frac{\partial Z}{\partial\eta} & - & - & - \\ - & - & - & - & - & - & \frac{\partial X}{\partial\tau} & \frac{\partial Y}{\partial\tau} & \frac{\partial Z}{\partial\tau} \\ \frac{\partial X}{\partial\tau} & \frac{\partial Y}{\partial\eta} & \frac{\partial Z}{\partial\eta} & \frac{\partial X}{\partial\zeta} & \frac{\partial Y}{\partial\zeta} & \frac{\partial Z}{\partial\zeta} & - & - & - \\ \frac{\partial X}{\partial\tau} & \frac{\partial Y}{\partial\tau} & \frac{\partial Z}{\partial\tau} & - & - & - & \frac{\partial X}{\partial\zeta} & \frac{\partial Y}{\partial\zeta} & \frac{\partial Z}{\partial\zeta} \\ - & - & - & \frac{\partial X}{\partial\tau} & \frac{\partial Y}{\partial\tau} & \frac{\partial Z}{\partial\tau} & \frac{\partial X}{\partial\eta} & \frac{\partial Y}{\partial\zeta} & \frac{\partial Z}{\partial\zeta} \end{bmatrix} \begin{Bmatrix} \frac{\partial u}{\partial X} \\ \frac{\partial u}{\partial Y} \\ \frac{\partial u}{\partial Z} \\ \frac{\partial v}{\partial X} \\ \frac{\partial v}{\partial Y} \\ \frac{\partial v}{\partial Z} \\ \frac{\partial w}{\partial X} \\ \frac{\partial w}{\partial Y} \\ \frac{\partial w}{\partial Z} \end{Bmatrix}$$

Jacobean 6×9

Finally every term in Jacobean matrix can expression as a shape function from Eq. (1).

I.e. $(x = N_1x_1 + N_2x_2 + N_3x_3 \dots\dots\dots N_8x_8)$,

So $\frac{\partial X}{\partial\zeta} = \frac{\partial N_1}{\partial\zeta}x_1 + \frac{\partial N_2}{\partial\zeta}x_2 + \frac{\partial N_3}{\partial\zeta}x_3 \dots + \frac{\partial N_8}{\partial\zeta}x_8$,

And by use the shape function derivatives Eq. (8) will be find all the independent.

Formulation of Mass Matrix

For anybody of infinitesimal mass dm and velocity vector $\{\dot{q}\}$, the kinetic energy [K, E] can be defined as:

$$K.E = \frac{1}{2}\int\{\dot{q}\}\{\dot{q}\}dm$$

But $dm = \rho dvol = \rho dxdydz$ Referring to Eq. (5) and relation $\{\dot{q}\} = [N]\{\dot{\delta}\}$;-

$$K.E = \frac{1}{2}\{\dot{\delta}\}^T[\iiint\rho[N]^T[N]dxdydz]\{\dot{\delta}\}$$

Then the element mass matrix can be written as:-

$$[M] = \iiint\rho[N]^T[N]dxdydz$$

Using the intrinsic coordinates the eq. can be written as:-

$$[M] = \rho\int_{-1}^{1}\int_{-1}^{1}\int_{-1}^{1}[N]^T[N]\,|J|\,d\zeta\,d\eta\,d\tau \qquad (16)$$

In which, ρ is the mass density

Determination of Damping Matrix

In general, the damping matrix may be of the form **[N. Ganesan and T. C. Ramesh, 1992]**;

$$[C] = [M]\sum_{i=1}^{m} a_i [[M]^{-1}[K]]^i \qquad (17)$$

Where m is the number of degrees of freedom.

$$\{a\} = 2[Q]^{-1}\{\zeta\} \qquad (18)$$

$$\{a\} = \begin{Bmatrix} a_1 \\ a_2 \\ \vdots \\ a_m \end{Bmatrix},$$

$$\{\zeta\} = \begin{Bmatrix} \zeta_1 \\ \zeta_2 \\ \vdots \\ \zeta_m \end{Bmatrix} \quad \&$$

$$[Q] = \begin{bmatrix} \omega_1 & \omega_1^3 & \omega_1^5 & \cdots & \cdots & \omega_1^{2m-1} \\ \omega_2 & \omega_2^3 & \omega_2^5 & \cdots & \cdots & \omega_2^{2m-1} \\ \vdots & \vdots & \vdots & \cdots & \cdots & \vdots \\ \omega_m & \omega_m^3 & \omega_m^5 & \cdots & \cdots & \omega_m^{2m-1} \end{bmatrix}$$

Where ω_1, ω_2 …ω_m are the natural frequencies of the system and ζ_1, ζ_2 …ζ_m are the damping ratios, by considering that the damping ratio is taken as (0.07) **[H. Vinayak, R. Singh, 1995].** Finally the damping matrix [C] is obtained by substituting Eq. (18) into Eq. (17).

SOLUTION OF FINITE ELEMENT EQUILIBRIUM EQUATION [Time History Analysis]

The general equation of motion can be written as **[Singireu S. Rao, 1967]**:-

$$[M]\{\ddot{U}\} + [C]\{\dot{U}\} + [K]\{U\} = \{R\} \qquad (19)$$

Where [M], [C] and [K] are mass, damping and stiffness matrices respectively, {R} is the external load vector; {U}, {$\dot{U}$} and {$\ddot{U}$} are the displacement, velocity and acceleration vectors respectively. All of them are being time–dependent. Therefore in dynamic analysis, in principles, static equilibrium at time (t), which includes the effect of acceleration dependent inertia forces and velocity-dependent damping forces, is considered. Time history analysis; is a technique used to determine the dynamic response of a structure under the action of any general time dependent loads. This analysis can be used to determine the time-varying displacement, strain, stresses and force in a structure as it responds to any type time dependent loads. So can be considering the Houbolt method is reference to a multi degree of freedom system **[Singireu S. Rao, 1967]**, the following finite difference expansions are employed;

$$\dot{x}_{i+1} = \frac{1}{6\Delta t}(11x_{i+1} - 18x_i + 9x_{i-1} - 2x_{i-2}) \qquad (20)$$

$$\ddot{x}_{i+1} = \frac{1}{(\Delta t)^2}(2x_{i+1} - 5x_i + 4x_{i-1} - x_{i-2}) \qquad (21)$$

To drive Eq. (20) & (21), consider the function (x_t). Let the values of x at the equally spaced grid points $t_{i-2}=t_{i-2}.\Delta t$, $t_{i-1}=t_i-\Delta t$, t_i and $t_{i+1}=t_i+\Delta t$ be given by x_{i-2}, x_{i-1}, x_i and x_{i+1} respectively, The Taylor`s series expansion, with backward step gives the following;

With step size=Δt;

$$x_{(i)} = x_{(i+1)} - \Delta t\,\dot{x}_{(i+1)} + \frac{1}{2!}(\Delta t)^2\ddot{x}_{(i+1)} - \frac{1}{6}(\Delta t)^3\dddot{x}_{(i+1)} \qquad (22)$$

With step size=$2\Delta t$;

$$x_{(i-1)} = x_{(i+1)} - 2\Delta t\,\dot{x}_{(i+1)} + 2(\Delta t)^2\ddot{x}_{(i+1)} - \frac{4}{3}(\Delta t)^3\dddot{x}_{(i+1)} \qquad (23)$$

With step size=$3\Delta t$;

$$x_{(i-2)} = x_{(i+1)} - 3\Delta t\,\dot{x}_{(i+1)} + \frac{9}{2}(\Delta t)^2\ddot{x}_{(i+1)} - \frac{9}{2}(\Delta t)^3\dddot{x}_{(i+1)} \qquad (24)$$

By considering terms up to $(\Delta t)^3$ only, Eq. (22) to (24) can be solved to express $\dot{x}_{(i+1)}$, $\ddot{x}_{(i+1)}$ and $\dddot{x}_{(i+1)}$ in terms of $x_{(i-2)}$, $x_{(i-1)}$, $x_{(i)}$ and $x_{(i+1)}$.

This gives $\dot{x}_{(i+1)}$ and $\ddot{x}_{(i+1)}$ as the Eq. of motion;

$$[M]\ddot{x} + [C]\dot{x} + [K]x = F.$$

And to find the solution at step i+1 ($x_{(i+1)}$), we consider Eq. of motion at t_{i+1}, so that;

$[M]\ddot{x}_{(i+1)} + [C]\dot{x}_{(i+1)} + [K]x_{(i+1)} = F_{(i+1)} = F\ (t = t_{i+1})$ (25)

By substituting Eq. (20) & (21) into Eq. (25), we obtain;

$$\left(\frac{2}{(\Delta t)^2}[M]+\frac{11}{6\Delta t}[C]+[K]\right)x_{(i+1)} = F_{(i+1)}+\left(\frac{5}{(\Delta t)^2}[M]+\frac{3}{\Delta t}[C]\right)x_{(i)}-\left(\frac{4}{(\Delta t)^2}[M]+\frac{3}{2\Delta t}[C]\right)x_{(i-1)}+\left(\frac{1}{(\Delta t)^2}[M]+\frac{1}{3\Delta t}[C]\right)x_{(i-2)} \quad (26)$$

A. Determine x_{-1} using Eq. (22).

B. Find x_1 and x_2 using the central difference relationship;

$$x_{(i+1)} = \left[\frac{1}{(\Delta t)^2}[M]+\frac{1}{2\Delta t}[C]\right]^{-1} \times \left[F_{(i)}-\left([K]-\frac{2}{(\Delta t)^2}[M]\right)x_{(i)}-\left(\frac{1}{(\Delta t)^2}[M]-\frac{1}{2\Delta t}[C]\right)x_{(i-1)}\right]$$

D. Compute x_{i+1}, starting with i=2 and using Eq. (26).

$$x_{(i+1)} = \left(\frac{2}{(\Delta t)^2}[M]+\frac{11}{6\Delta t}[C]+[K]\right)^{-1} \times \left\{F_{(i+1)}+\left(\frac{5}{(\Delta t)^2}[M]+\frac{3}{\Delta t}[C]\right)x_{(i)}-\left(\frac{4}{(\Delta t)^2}[M]+\frac{3}{2\Delta t}[C]\right)x_{(i-1)}+\left(\frac{1}{(\Delta t)^2}[M]+\frac{1}{3\Delta t}[C]\right)x_{(i-2)}\right\}$$

The step-by-step procedure to be used in the Houbolt method is giving below;

Form the known initial conditions at t=0 x_0 and $\dot{x}_0$ to find $\ddot{x}_0$ by using Eq. of motion;

$\ddot{x}_0 = [M]^{-1}(f_0 - [C]\dot{x}_0 - [K]x_0)$.

C Select a suitable time of step Δt.

FORMULATION OF GLOBAL MATRICES & IT`S EVALUATION

The individual element stiffness's were assembled in the usual way. The global stiffness matrix was of size 24×24. The half band width was obtained.

A uniform load of 245.25 N/mm was assumed to act at the tip as shown in Fig. 1 those of mild steel gear. The trend of these variations indicates that orthotropic material gears also behave similarly to isotropic material gears.

The maximum stress near the root along the fiber is 10% and 21.5% more for this uniformly distributed load was lumped at the nodes.

Strategy for Determining the Stiffness Matrix

A. Compute the nodal coordinate in the real element in meters {in this work we have just (68) nod in x-y plane and (340) nod for holly tooth body}

B. Form strain displacement matrix [B], by apply the master element coordinate (ζ,η,τ) of the gauss point use Eq. (8) to find the independent of Eq. (7).

Differentiation of Eq. (1) with respect to (ζ, η, and τ) and put the shape function derivatives formula Eq. (8), to create the Jacobean matrix. Integrate the stiffness formula Eq. (15) by gauss four point to form matrix of size 24×24.

Strategy for Determining the Inertia & Damping Matrix

A. Integrate by gauss quadratic formula Eq. (16) but the value of mass to be in term of density depending on the type of the orthotropic material that use.

B. Apply the natural frequencies, the mass matrix, and damping ratio in Eq. (17), to determine the damping matrix for each material that considered in the current work.

DISCUSSION

Static Analysis

It was observed that the variations of displacements U, V, W, the normal stresses in L, T, Z directions, and the shear stresses in the LT, TZ, ZL planes both along the involute profile on the load surface and across the root

Gl/Ep and Gr/Ep than the Ms Gear, Fig. 5-a. Whereas, the maximum stresses, in the other two directions, are very much lower. In the T direction it is 56% and 70% less Fig. 5-b. And in the Z -direction 74% and 87% less for

Gl/Ep and Gr/Ep gears respectively than Ms gear Fig. 5-c.

Similarly the shear stresses near the root in the LT plane, for orthotropic material gears is much less than that of isotropic gear, even though at the tip they are 24.5% and 43% more for Gl/Ep and Gr/Ep than Ms gear Fig. 6-a. The shear stress, in the other two planes TZ and ZL, even though the graph indicates some amount of dispersion, magnitude wise they are negligibly small Fig. 6-b and Fig. 6-c. All the figure shown the variations of stresses along the gear tooth profile on the load surface

It is reported by many investigators that the stresses on the compression side of the gear tooth are slightly more than those on the tension side **[Lewis, W., 1892]**. In this investigation also, along the fiber orientation direction, for Ms-Gear the maximum compressive stress is 11.75% more than the maximum tensile stress, whereas the maximum compressive stress is only 7% and 0.3% for Gl/Ep and Gr/Ep gears. These variations are shown in Fig. 7-a, Fig. 7-b, Fig. 7-c, Fig. 7-d, Fig. 7-e, Fig. 7-f.

Although the stresses are in a favorable direction, the displacements are relatively large for orthotropic materials. At the critical section, displacement U in the radial (L) direction is 7.5 times larger and 2.16 times larger Fig. 8-a. And displacement V in the tangential (T) direction is 11.6 times and 5.3 times larger Fig. 8-b. For the Gl/Ep and Gr/Ep gears than their corresponding values for the Ms gear.

The displacements W in (Z) direction along the face width of the gear are negligibly small in all the three cases as they are of the order of 10^{-6} Fig. 8-c.

In a similar way the displacements across the root thickness are also more for Gl/Ep and Gr/Ep gears. This is shown on Fig. 9-a, Fig. 9-b, and Fig. 9-c.

From Fig. 5 to Fig. 9 it may be observed that the performance of Gr/Ep gear is very much closer to Ms-Gear than Gl/Ep gear. Hence it may be concluded that Gr/Ep is a better material compared to Gl/Ep as an alternate for Ms for power transmission gears.

Dynamic {Time History} Analysis

The evaluation of dynamic stresses present by using maple calculator to solve the finite element equation motion for transient dynamic analysis and their procedures of the eigenvalues and eigenvectors for various modes wear obtained. These eigenvalues and eigenvector were then used in anther calculation {Houbolt method} in which the mode superposition technique was used to evaluate the dynamic stresses. The dynamic loads that act on the gear tooth sector can be considered as ***one half of a sinusoidal type impulse load*** Fig. 2 which represented by **[Kazunor, 1974];-** $F_t = F \sin\left(\frac{\pi t}{tf}\right)$

A- Time History Analysis of Concentrated Load on the Tip of the Gear Tooth

One half of a sinusoidal type impulse load will be concentrated in the tip of the gear tooth as shown in Fig.3 to studies the decay of vibration of the gear tooth, from calculate the displacement and stresses were carried out for (90-micro-sec) with (1.8- micro-sec) time step.

B- Time History Analysis of Moving Line Load on Gear Tooth Profile

The maximum normal load F_n acting on the gear tooth sector was assumed to be 245.25 N per mm length of face width. The load distribution on the tooth profile, when the load moved from the tip to the bottom, was assumed to be of the form shown in Fig. 4 in accordance with the theory of gearing **[Ramamurti, V., and Ananda, M., 1988]**.this normal load was considered in terms of its components in the radial and tangential direction with account taken of the pressure angle at any point under consideration; that is, the tangential load is

$F_t=F_n \cos \alpha_i$ And the radial load is $F_r=F_n \cos \alpha_i$, where α_i is the pressure angle at the point under consideration.

Discussion of Time History Analysis for Concentrated Load Response

The time history of tooth tip displacement for two types of spur gears made of composite material (Gl/Ep and Gr/Ep), represent low dynamic response in there modes shape with respect to mild steel gear, where the maximum deflection in the tip is (33%) and (16.6%) less for Gl/Ep and Gr/Ep than the Ms Gear Fig. 10-a, whereas, the maximum deflection in the other two

directions, are very much lower Fig. 10-b, and Fig. 10-c.

The maximum fillet stress along the fiber direction (σ_L) is (38%) and (41.5%) more for Gl/Ep and Gr/Ep than the Ms Gear, whereas, the maximum stresses, in the other two directions, are slightly more. In the (σ_T) direction it is (21%) and (28%) more .And in the (σ_Z) direction (11%) and (16%) more for Gl/Ep and Gr/Ep gears respectively than Ms gear Fig. 11.

Similarly the shear fillet stresses in the (τ_{TZ}) plane, they are (35%) and (20%) more for Gl/Ep and Gr/Ep than Ms gear. The shear stress, in the other two planes (τ_{LT})and (τ_{ZL}), even though the graph indicates some amount of deference's between the orthotropic gears and isotropic one in the magnitude these shear stresses wise they are negligibly small Fig. 12.

Recorded that the amplitude of dynamic displacement exceeds the static displacement by (48%), (60%) for Gl/Ep and Gr/Ep respectively for application of sinusoidal concentrated load. In a similar way the dynamic stresses exceeds the static stresses by (20%), (35%) for Gl/Ep and Gr/Ep respectively for the same application of load.

Discussion of Time History Analysis for Moving Line Load Response

The total time taken for the load to move from top to bottom was obtained as (6.25×10^{-3}) Sec. **[K. J. Huang, and T. S. LIU, 2000]**. This time was divided into **1000** intervals, each of (6.25) μs, the proportionate number of intervals during which the load moves form one node to the other was calculated. The load was moved down the profile at each interval of (6.25) μs and the corresponding loads shared by the adjacent nodes were calculated. Thus the new load vector for each interval was calculated and fed into the dynamic calculation by use of Houbolt method, and the corresponding respectively, but for the isotropic material Ms is 84.372Mpa Fig. 13, but the root stresses under static load condition for the same cases is 122.72Mpa, 101.36Mpa, 87.52Mpa for Ms, Gr/Ep, and Gl/Ep respectively, which is more than the dynamic load condition. The reason is that in the static analysis case the full load was assumed to act at the tip, whereas in the case of dynamic analysis only half of the load acts at the tip.

When the full load at the tip is considered as a moving load then the corresponding maximum dynamic root stresses obtained was 194.95Mpa, 183.72Mpa, and 164.19Mpa for Ms, Gr/Ep, and Gl/Ep respectively [by put the equivalent load in the tip of the tooth profile].

Also the mode shape of the point on the tip will be calculated for Ms, Gr/Ep, and Gl/Ep in Fig. 14-a, Fig. 14-b, and Fig. 14-c, which represent the deformation of the tooth tip under the moving line of load. thickness for the two orthotropic material gears were very similar to

displacements and stresses were thus obtained.

It is reported by many investigators that the variation of dynamic root stresses with time to that the dynamic stresses at the root

when the load is at the tip is less, and greater when the load is at the mid-height. This is obvious since the dynamic stresses is greater when the full load is impressed on only one tooth, even though the bending moment arm is slightly less.

In this work will be found that the peak stresses for two orthotropic materials Gl/Ep and Gr/Ep is 98.468Mpa and 75.719Mpa

CONCLUSION

1. The behavior of orthotropic material gears and mild steel gears (i.e. the variations of stresses and displacements both along tooth profile and across the tooth thickness) are very similar.
2. The maximum normal stress in the fibre (L) direction in orthotropic material gears is little more than the maximum stress in mild steel gear.
3. The maximum normal stresses in the other two perpendicular (T and Z***)*** directions for orthotropic material gears are much smaller than that of mild steel gear.
4. The shear stress in the LT plane alone for orthotropic material gears is slightly more than that for mild steel gear, whereas the other two perpendicular (TZ and ZL) planes are negligibly less.
5. The displacements in the radial and tangential directions of orthotropic material gears are considerably more than that of mild steel gear, even along the face width it is almost zero.
6. For orthotropic material gears the maximum stress decreases with decreasing rim thickness, in the range of analysis made.
7. The Ms gear represent more response respect to the concentrated dynamic load then the Gl/Ep and Gr/Ep gears where it gives a little mode shapes and natural frequencies values for same load
8. The amplitude of dynamic stresses exceeds the static stresses for sinusoidal concentrated load.
9. The peak root stresses inhibit in the gear tooth that made of composite material respect to the dynamic moving load on the surface profile is slightly less than the concentrated load on tip.
10. Also that is found the spur gear that made from composite (graphite/epoxy) also comes very much closer to mild steel gear behavior, may definitely be thought of for power transmission.

REFERENCES

H. Vinayak, R. Singh, and C. Padmanabhan, (Linear Dynamic Analysis of Multi-Mesh Transmission Containing External, Rigid Gear) Journal of Sound and Vibration (1995) 185(1) 1-32.

Jean-Marie Berthelot, (Mechanical Behaviour of Composite Materials and Structures), Book ISMANS Institute for Advanced Le Mans, France Materials and Mechanics.

Kazunori and Fujio, (Dynamic Behavior of Heavy-Loaded Spur Gears), Transaction of ASME, Journal of Engineering for Industry, PP.373-381, May 1974.

K. J. Huang, and T. S. LIU, (Dynamic Analysis of A Spur Gear by the Dynamic Stiffness Method), Journal of Sound and Vibration (2000) 234(2), 311)329; http://www.idealibrary.com

Lewis, W., (Investigation of the Strength of Gear Teeth), Proceeding Engineers, Club, Philadelphia, October 1892.

N. Ganesan and T. C. Ramesh, (Free Vibration Analysis of Composite Wheels), Journal of Sound and Vibration (1992) 153(l), I13-124, Elsevier Science Publishers Ltd.

Ramamurti, V., and Ananda, M., (Dynamic 1988.

Singireu S. Rao, (Mechanical Vibrations)

Analysis of Spur Gear Teeth), Indian Institute of Technology, India, Journal of Computers and Structures, Vol.29, No.5, PP.831-843,

Third Edition, Addiso-Wesley Publishing Company

S. Mohamed Nabi & N. Ganesan, (Static Stress Analysis of Composite Spur Gears Using 3D-Finite Element and Cyclic Symmetric Approach), Composite & Structures Vol. 46, No. 5, pp. 1993

Toshiki H., Eiichi A. Tsutao K. (Development of Design System for Composite Gears for Power Transmission), 2006 Elsevier, Science Direct, Japan Doshisha Univ.

Vijayarangan and N. Ganesan ,(Stress Analysis of Composite Spur Gears Using 3D-Finite Element Approach), Computers & Structures Vol. 46, No. 5, pp. 869475, 1993 Elsevier Science ltd.

Table 1 gear tooth parameter.

NO.	Design Parameter	Value
1.	Pressure angle	20^o
2.	Module , mm	10
3.	Addendum	1m
4.	Dedendum	$1.25m_o$
5.	Root fillet radius	$0.3m_o$
6.	Rim thickness	$1.25m_o$
7.	Number of teeth	20
8.	Face width	$11m_o$
9.	Loading Condition	$\beta=31.1684^o$

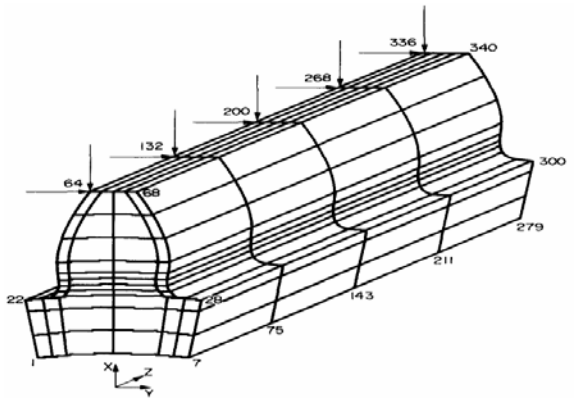

Fig. 1 gear meshing and tooth sector.

Table 2 mechanical properties for studying case.

PROPERTIES		MS	Gl//Ep	Gr/Ep
1.	E_1,N/mm^2	20.60100	37.86660	180.99450
2.	E_2,N/mm^2	20.60100	8.11290	10.70270
3.	E_3,N/mm^2	20.60100	8.09990	10.51276
4.	G_{12},N/mm^2	79.2354	4.06130	7171.10
5.	G_{13},N/mm^2	79.2354	1.07711	0.90724
6.	G_{23},N/mm^2	79.2354	1.12361	0.91132
7.	ν_{12}	0.3	0.26	0.28
8.	ν_{12}	0.3	0.0366	0.11
9.	ν_{12}	0.3	0.0363	0.105
10.	Density,Kg/mm^2	781E-10	1.81E-10	1.46E-10
11.	X_T,N/mm^2	353.2	981.00	1079.10
12.	Y_T,N/mm^2	353.2	34.40	34.40
13.	Z_T,N/mm^2	353.2	40.87	42.54
14.	S,N/mm^2	176.6	88.30	88.30
15.	ν_{21}	Isotropic	0.065	0.0167
16.	ν_{13}		0.009	0.0063
17.	ν_{32}		0.036	0.103
18.The weight of model		9.413547	3.7674	2.2135

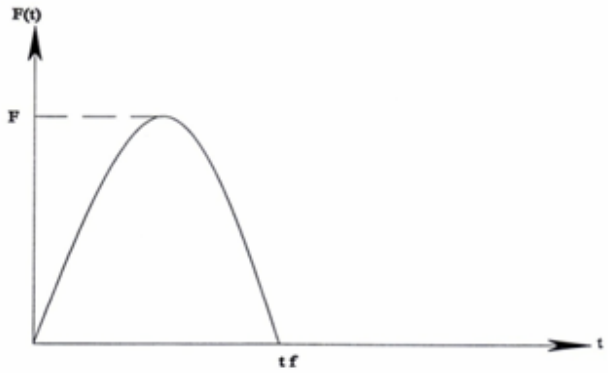

Fig. 2 The time history of one half of sinusoidal type impulse loads.
F=Amplitude of the applied load
F= (245.25 N) per (mm) of tooth face width.
tf =Total duration of the load, which is taken as (30) microsecond.

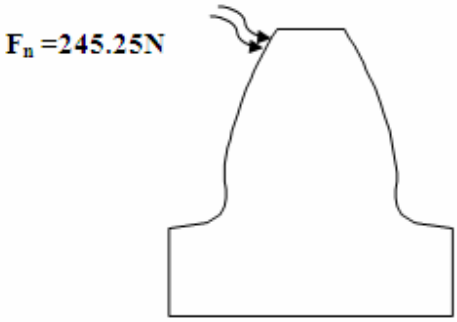

Fig. 3 one half sinusoidal type impulse concentrated load.

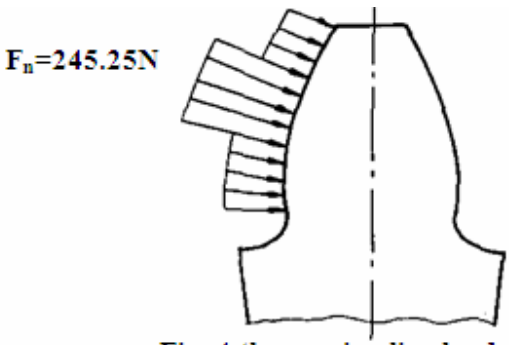

Fig. 4 the moving line load on tooth profile.

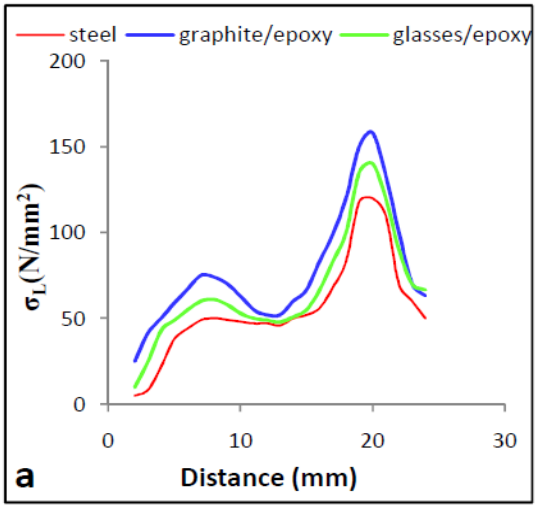

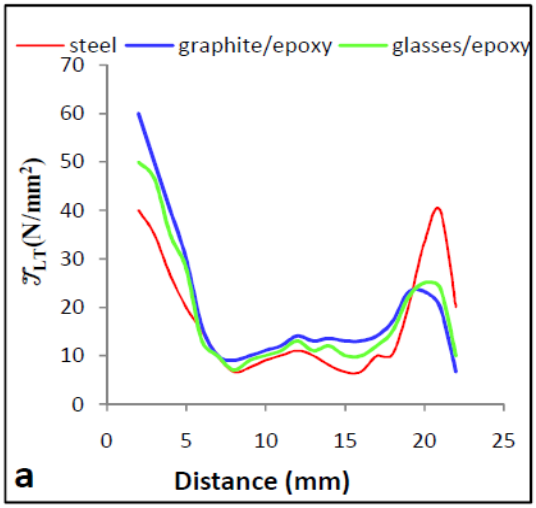

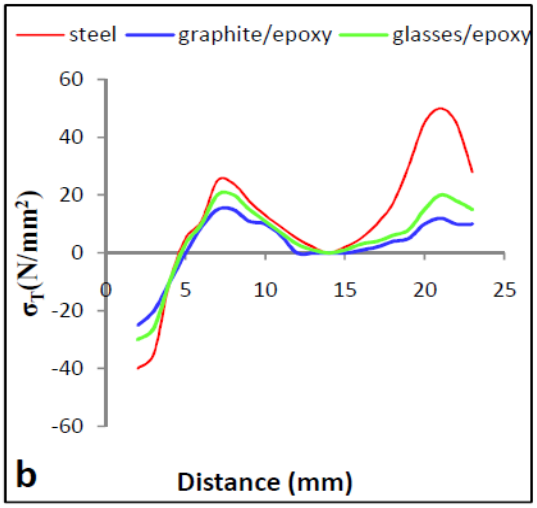

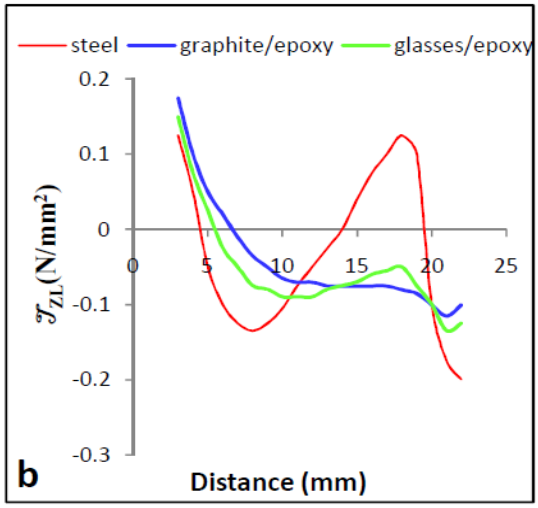

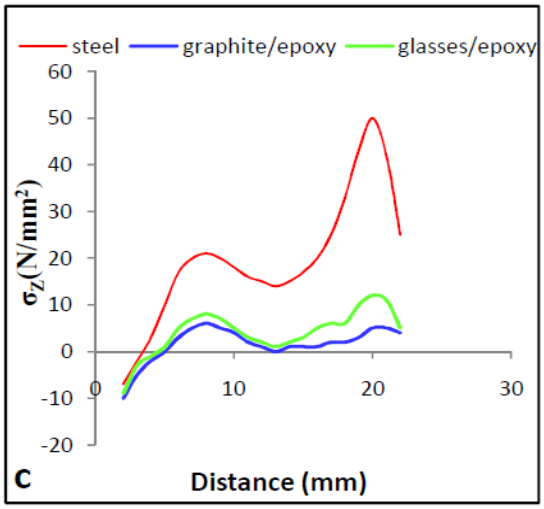

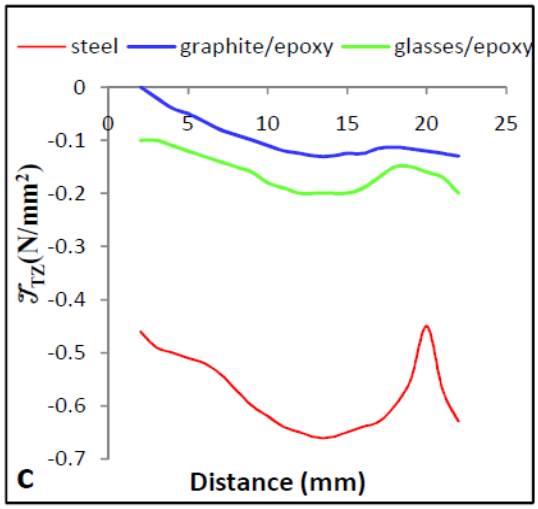

Fig. 5.a-b-c the maximum stress near the root.

Fig. 6.a-b-c the shear stresses near the root.

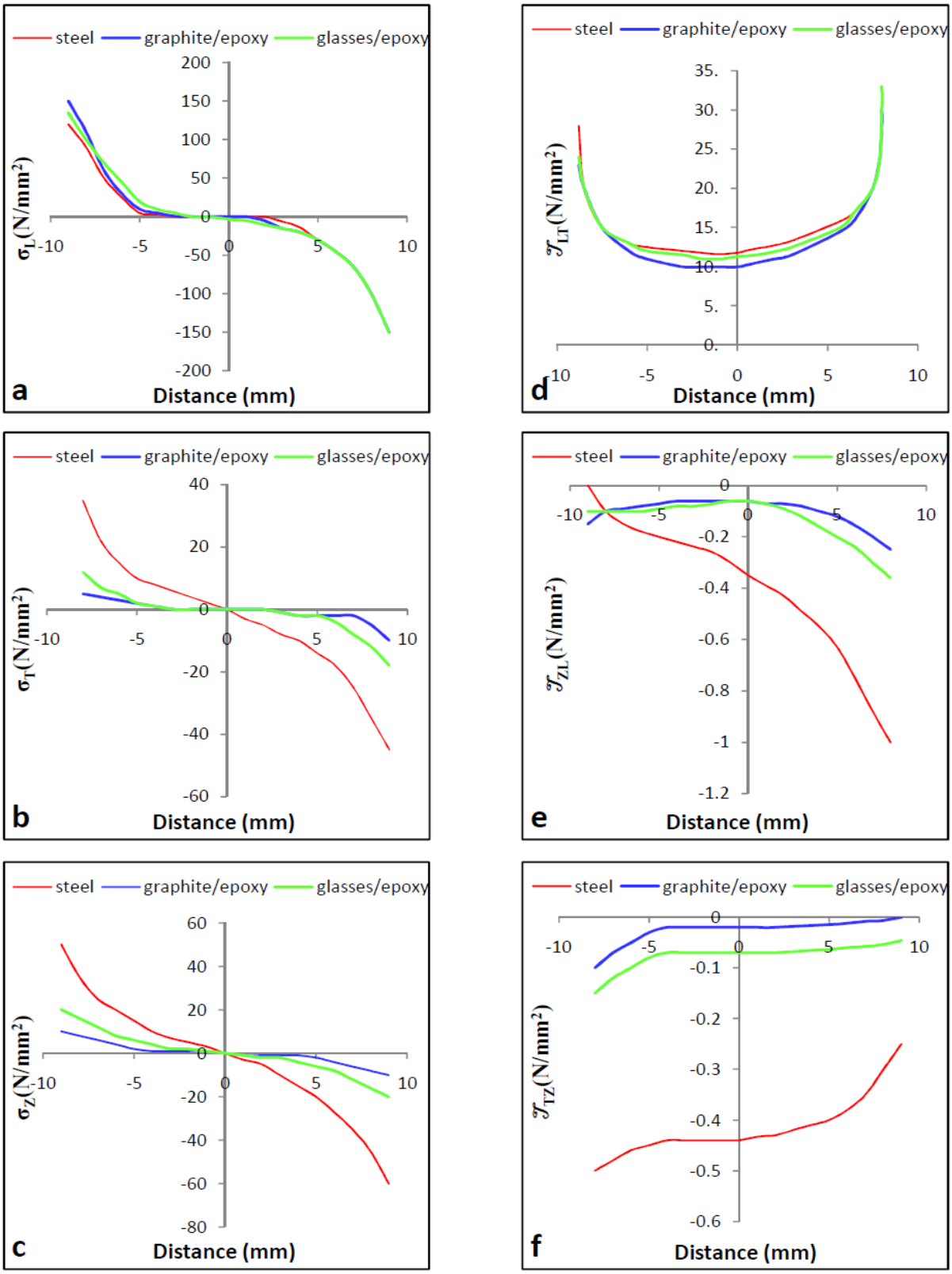

Fig. 7.a-b-c-d-e-f maximum stresses a cross root thickness.

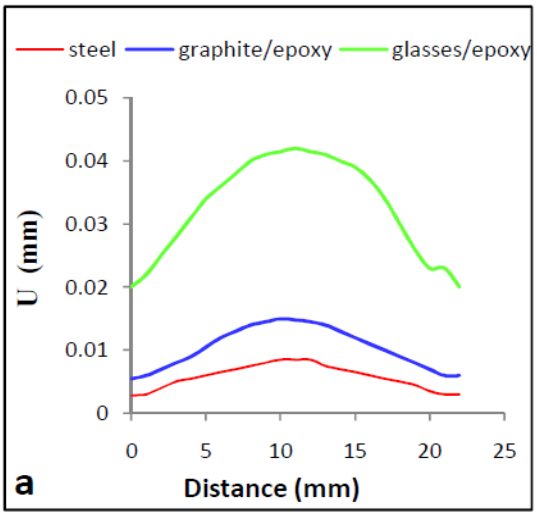

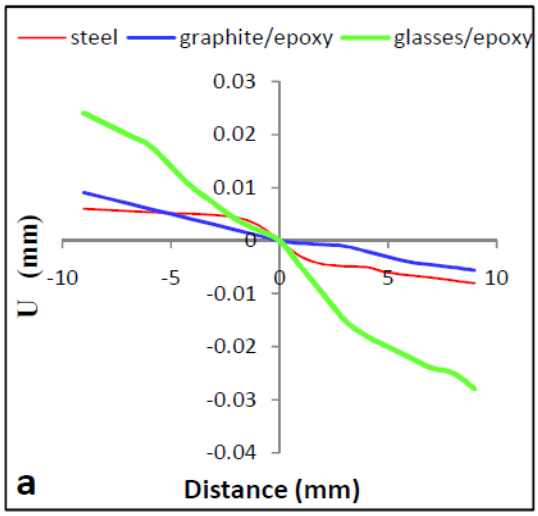

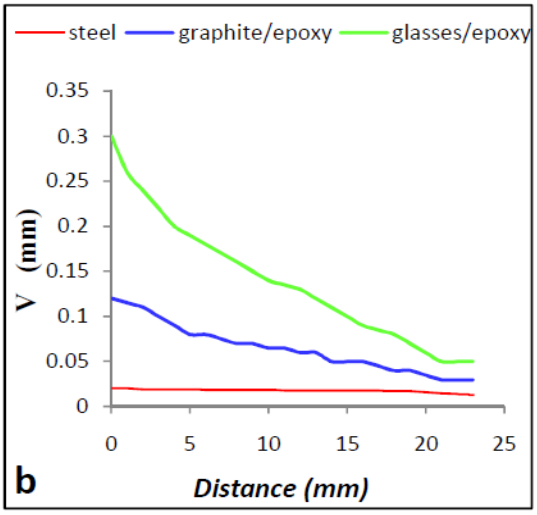

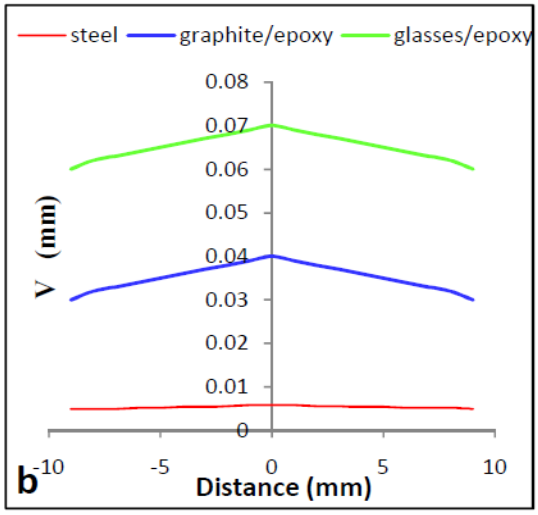

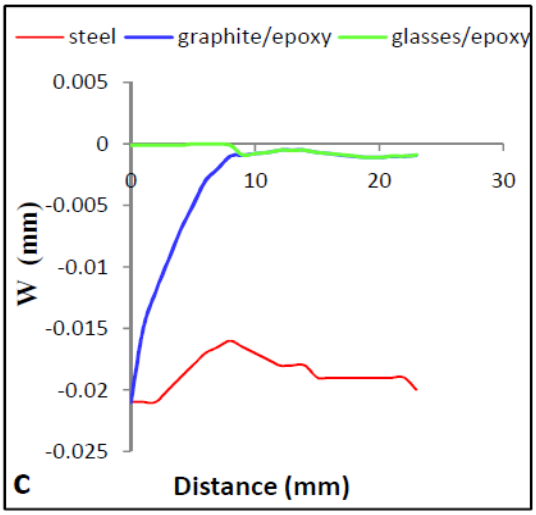

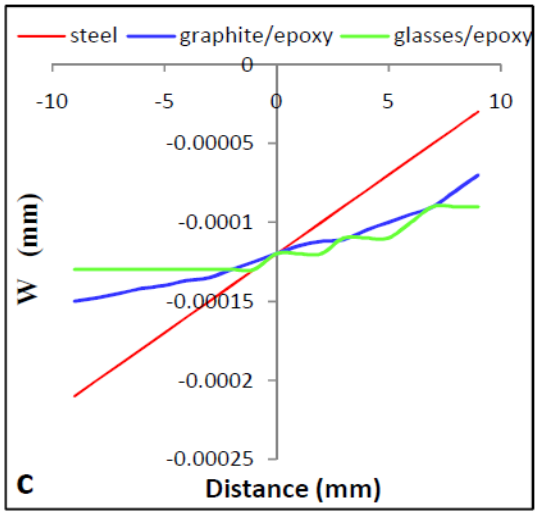

Fig. 8.a-b-c displacement along surface profile. **Fig. 9.a-b-c displacement a cross root thickness.**

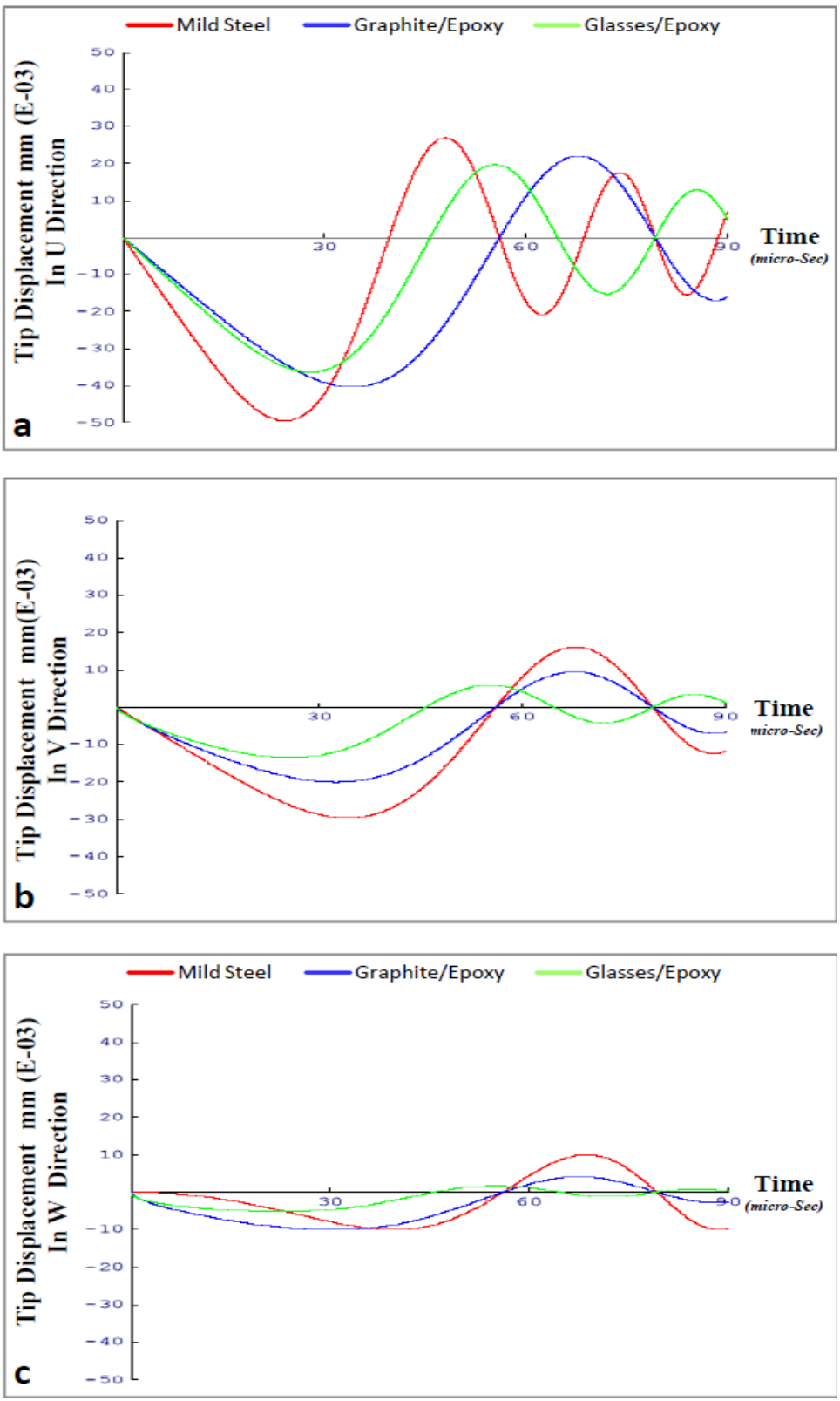

Fig. 10.a-b-c the maximum deflection in the tip

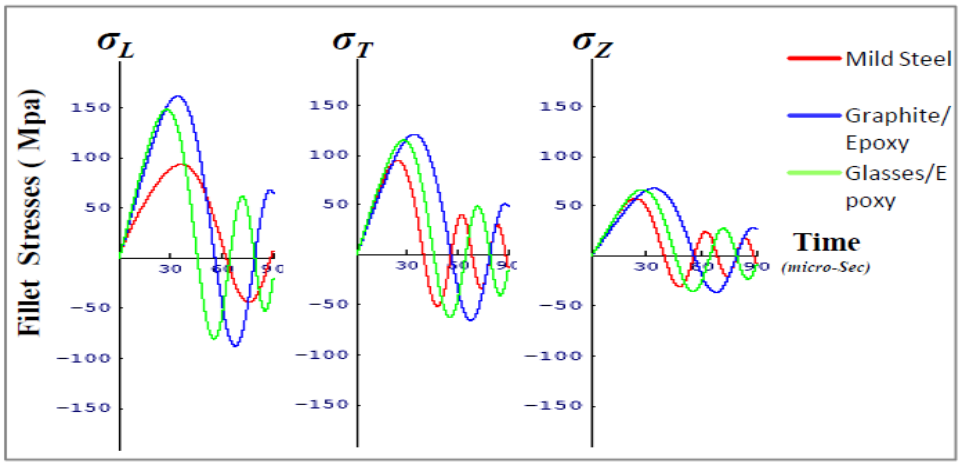

Fig. 11 fillet normal stresses due to the sinusoidal conetrated load.

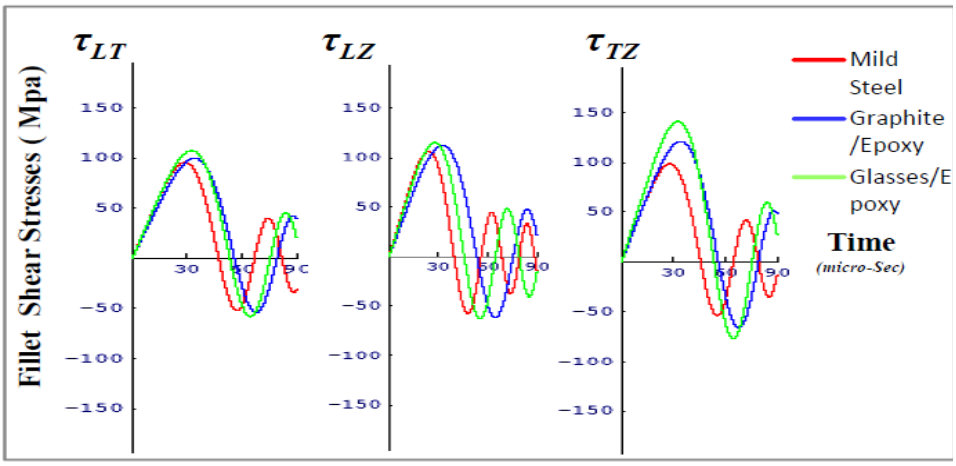

Fig. 12 fillet shear stresses due to the sinusoidal conetrated load.

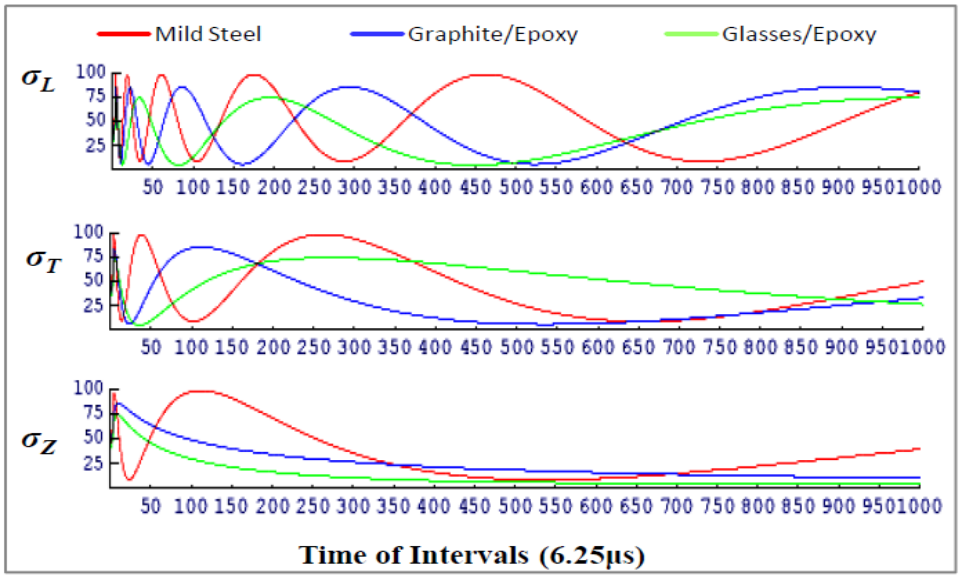

Fig. 13 fillet stresses due to the moving line load.

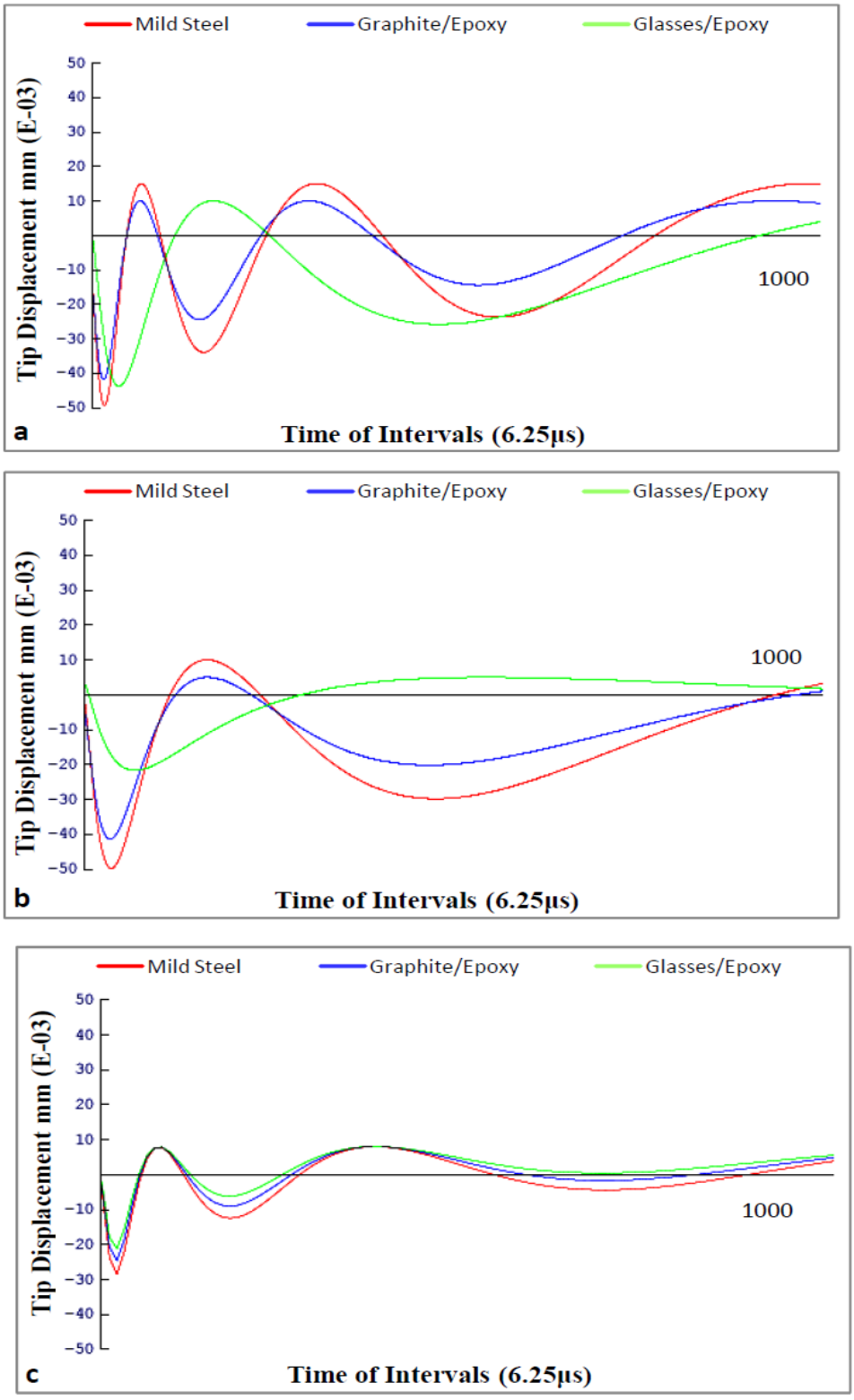

Fig. 14.a-b-c the mode shape of the gear tooth tip in W direction.